

## Neutrino Astrophysics

---

**Piero Galeotti\***

*Dept. of Physics, University of Torino, Italy*

*E-mail: [piero.galeotti@unito.it](mailto:piero.galeotti@unito.it)*

**Iskya García**

*Universidad Central de Venezuela, Venezuela.*

*E-mail: [giskya@gmail.com](mailto:giskya@gmail.com)*

**Cynthia Contreras**

*Comisión Nacional de Investigación y Desarrollo Aeroespacial, Peru.*

*E-mail: [cynthia.contreras14@gmail.com](mailto:cynthia.contreras14@gmail.com)*

In this lecture we discuss some fundamental aspects of neutrino astrophysics, in particular solar and supernova neutrinos

*4th School on Cosmic Rays and Astrophysics,  
August 25- September 04, 2010  
Sao Paulo Brazil*

---

\*Speaker.

## 1. Introduction and neutrino properties

In the 1920s, physicists noticed some discrepancies in beta decay experiments. A neutron decays into a proton by emitting an electron. It was observed that the total momentum and energy of the electron and proton after the decay was sometimes less than the initial momentum and energy of the neutron. In 1930, Wolfgang Pauli suggested the idea of neutrinos as the particles that carry away the missing energy, and at the same time opened the doors for the today neutrinos as particles of the Standard Model.

Neutrinos are extremely light particles, they have no electric charge and interacts only through the weak force. For this reason, neutrino interactions with matter are extremely rare, and they are difficult to detect; nevertheless in 1956 F. Reines and C. L. Cowan finally succeeded in detecting neutrinos produced by the Savannah River Nuclear Reactor. In 1957 Bruno Pontecorvo was the first to propose the concept of neutrino oscillations and later presented the first intuitive understanding of two neutrino mixing angles and oscillations. By 1962, a particle accelerator at Brookhaven National Laboratory was generating enough neutrinos to make detection experiments. Then physicists observed neutrino events and found evidence of two types of neutrinos. The first one discovered was the electron neutrino, and the second the muon neutrino. Proof of a suspected third type of neutrino, the tau neutrino, were found in late 1998.

Nowadays large neutrino detection experiments have developed all around the world, with different purposes like detect neutrino oscillation, solar and supernova neutrinos, atmospheric neutrinos and the detection of the three types of neutrinos. Some of the presently running experiments are SuperKamiokande, KamLand and T2K in Japan, LVD, Borexino, Opera and Icarus in Italy, Antares in France, SNO in Canada, Ice Cube in Antarctica, Minos in USA, Baikal in Russia, etc.

The Standard Model of particle physics contains three left-handed neutrino types which interacts through the weak force, namely  $\nu_e$ ,  $\nu_\mu$  and  $\nu_\tau$ , each describing a left-handed fermion (right-handed antifermion) with spin  $1/2$  like any lepton. These Standard Model are strictly massless by global chiral lepton number symmetry.

However, neutrino oscillation data have provided compelling evidence that at least one of the neutrino species has non-zero mass. This raises several theoretical and phenomenological issues that were not present for the case of massless neutrino predicted by the Standard Model.

One of the issue that brings the nature of the neutrino mass is that it could be a Majorana or a Dirac mass type, the first being the case when a neutrinos is its own antiparticle and the second case when it is not. Other issues are neutrino mixing and oscillations that represent a strong evidence for neutrinos be massive.

We know that neutrinos are left-handed particles and, if the neutrino were massless as suggested by the Standard Model, the chirality is a relativistic invariant. In other words, if neutrinos have non-zero mass, it is possible to construct a reference system where neutrinos are right-handed. However, in this case we cannot know if it is a neutrino or an antineutrino because of the lack of electric charge. But again, we know that in nature right-handed antineutrinos exist, and it is possible to construct another reference system where a second observer see a right-handed field, while we see a left-handed field.

In this case we have four independent degrees of freedom, and we can state that the neutrino is a Dirac particle; the only way to establish the difference between neutrinos and antineutrinos is due

the leptonic number associated with a global symmetry. However, this symmetry is a consequence of the dynamics and the field involved in the Standard Model. So, if the lepton number is not conserved, there is no reason for the neutrino and antineutrino fields to become the same under Lorentz transformation; it means that there is the possibility that the spinor associated with the neutrino could be represented by two degrees of freedom, and this is called the Majorana field.

Summarizing, if we made a change in the reference system of a particle, we get its antiparticle (Dirac). Which seems contradictory, because the charge is a Lorentz invariant; but in this case we make reference to conserved quantities that allow us to distinguish between the two states; and if it is not conserved, a particle could be equal to its antiparticle (Majorana) (Fig1).

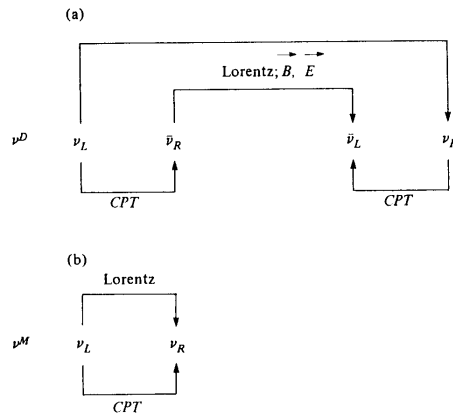


Figure 1: a)Dirac or b)Majorana neutrino.

Neutrinos are mainly produced in experiments by charged current weak interaction and, if neutrino mixing does exist, the charged current can produce any neutrino together with a charged lepton. As a consequence, a neutrino beam is a superposition of different particles eigen states and, as the beam propagates, different components of this beam evolve differently, so that the probability of finding different eigenstates in the beam varies with time. This consequence of neutrino mixing, is called neutrino oscillation (Fig2).

Pontecorvo suggested that the flavor eigenstates  $\nu_\alpha (\alpha = e, \mu, \tau)$  are linear combination of the mass eigenstates  $\nu_i (i = 1, 2, 3)$ , namely:

$$| \nu_\alpha \rangle = \sum_i U_{\alpha i} | \nu_i \rangle$$

Considering only two neutrino families for simplicity, we have:

$$\begin{pmatrix} \nu_\mu \\ \nu_e \end{pmatrix} = \begin{pmatrix} \cos \theta & \sin \theta \\ -\sin \theta & \cos \theta \end{pmatrix} \begin{pmatrix} \nu_1 \\ \nu_2 \end{pmatrix} \tag{1.1}$$

where  $\theta$  is the mixing angle.

A eigenstate  $| \nu_\alpha \rangle$  created in a process together with a weak charged lepton of the same species, can evolve in time to mixing in another state  $| \nu_\beta \rangle$ ; the processes can be  $\nu_\alpha \leftrightarrow \nu_\beta$  and  $\bar{\nu}_\alpha \leftrightarrow \bar{\nu}_\beta$ , while the transition  $\nu_\alpha \leftrightarrow \bar{\nu}_\beta$ , has less probability to occur because it also requires the change of helicity, that is proportional to  $\frac{m_\nu}{E_\nu}$ .

To examine the phenomenological characteristics of neutrino oscillations, consider a beam of neutrinos at constant momentum  $p_\nu$  and mass  $m_i \ll p_\nu$  moving along the X axis with total energy:

$$E_i = (p_\nu^2 + m_i^2)^{\frac{1}{2}} \approx p_\nu + \frac{m_i^2}{2p_\nu} \quad (1.2)$$

Assuming the neutrino beam originates at time  $t = 0$  in position  $x = 0$  in a weak process in which a charged lepton (or antilepton) is absorbed, or charged antilepton (or lepton) is created, the corresponding wave equation is:

$$\Psi_{(x,t)} = \sum_i U_{li} e^{ip_\nu x} e^{-iE_i t} \mathbf{v}_i \approx e^{ip_\nu(x-t)} \sum_i U_{li} e^{-i \frac{m_i^2}{2p_\nu} t} \mathbf{v}_i \quad (1.3)$$

An observer placed at distance  $L = x$  from the source, has a probability proportional to  $|\Psi\Psi^*|$  to observe the neutrino beam that if oscillations occur, it will not be pure anymore, but composed of neutrinos eigenstates of mass  $m_1$  and  $m_2$ . The oscillation probability is proportional to:

$$P \propto \exp\left[i \frac{(m_1^2) - (m_2^2)}{2p_\nu} L\right] \quad (1.4)$$

and indicates that a phase difference  $\frac{\Delta m^2 t}{2p_\nu} = \frac{\Delta m^2 L}{2p_\nu}$ , where  $\Delta m^2$  is generated over time (or along the way). Then the observed signal varies periodically with the distance of the detector from the source, repeating for integer multiples of the oscillation length, which is obtained by placing the phase  $\phi = 2\pi$ , in the following equation.

$$L_{osc} = 2\pi \frac{2p_\nu}{(m_1^2 - m_2^2)} = 2,48 K m \frac{E_\nu (GeV)}{\Delta m^2 (eV^2)} \quad (1.5)$$

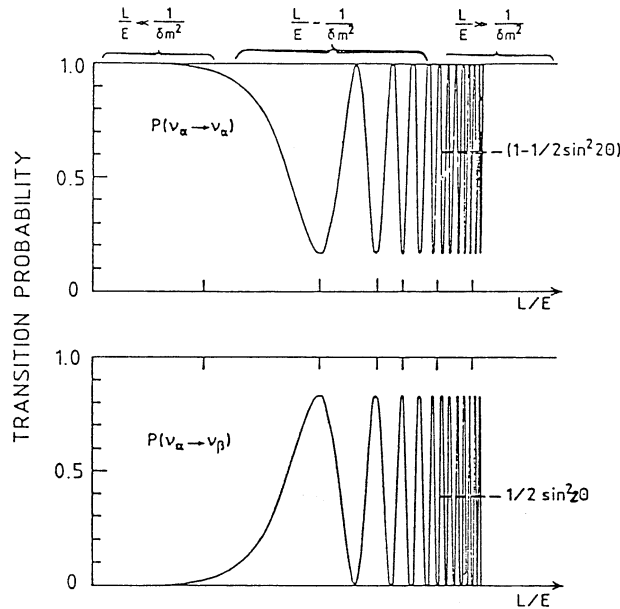


**Figure 2:** Oscillation probability of the neutrino in function of  $\frac{L}{E}$

Finally, if neutrinos are massive they could have a magnetic moment. In this case, neutrinos could change helicity from left-handed to right-handed, and become sterile and not detectable in weak interaction processes, while crossing regions with enough intense magnetic field component perpendicular to their direction of motion. According to Standard Model, the neutrino magnetic moment is:

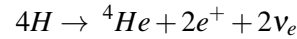
$$\mu_\nu = \frac{3eG_f}{8\sqrt{2}\pi^2} m_\nu = 3,2 \cdot 10^{-19} \mu_B \left( \frac{m_\nu}{eV} \right) \quad (1.6)$$

where  $\mu_B$  is the Bohr magneton.

## 2. Solar neutrinos

Considering the Sun as an ideal gas in hydrostatic equilibrium, we can get all its internal characteristics, such as density and temperature, from which thermonuclear reaction rates of hydrogen burning into helium can be evaluated. This process explain the long life of stars, and the neutrino production.

The dominant thermonuclear reaction inside the Sun is given by:

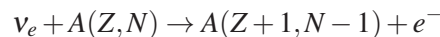


The total energy released in this process is 26.7 MeV; part of it is immediately emitted as neutrinos, the rest as high energy photons produced directly in the reaction and in positron annihilation  $e^+ + e^- \rightarrow 2\gamma$ . These photons, with average energy about 10 MeV, diffuse to the Sun atmosphere, are thermalized and emitted as low energy photons with a black body distribution, producing of order of ten millions photons with average energy  $\sim 1eV$  emitted from the solar photosphere.

The total number of thermonuclear reactions in the core should produce as much energy as that emitted by the solar photosphere in order to justify the solar luminosity  $L_\odot = 4 \cdot 10^{33} \text{ergs}^{-1}$ , which constitutes a strong constraint to the reaction rate of hydrogen burning in the solar interior. Since each proton releases about  $7MeV \sim 10^{-5} \text{erg}$  of energy, it follows immediately that the hydrogen must be burned at the rate of  $4 \cdot 10^{38} \text{protons} \cdot s^{-1}$ . Consequently, the rate of neutrinos emitted by the Sun is  $2 \cdot 10^{38} s^{-1}$  and, from the value of the Earth-Sun distance, the corresponding neutrino flux at Earth is of the order of  $10^{15} \nu_e m^{-2} s^{-1}$ .

From the definition of the mean free path, we obtain the value  $\chi_f \sim 10^{-3} m$  for photons and  $\chi_\nu \sim 10^{18} m$  for neutrinos. Therefore, while the photons spread slowly to the surface of the Sun, with a delay of more than  $10^{12} s (10^5 \text{years})$ , neutrinos escape immediately from the Sun and after about 8 minutes reach the Earth, where are detectable in underground detectors. The specific reactions producing neutrinos in the Sun and their characteristics are given in table 2 and the spectrum is shown in figure 3.

Solar neutrinos are detected by capture processes in nuclei:



Among the many nuclei proposed to measure the neutrino flux the first experiment used  ${}^{37}Cl$  which turns into  ${}^{37}Ar$ , later Ge was used in the reaction  ${}^{71}Ge \rightarrow {}^{71}Ga$ . The chlorine experiment,

Reaction	$E_\nu$	$E_\nu$	Flux to the Earth ( $\nu_e cm^{-2} s^{-1}$ )	
	max. (MeV)	average (MeV)	minimum	maximum
$p + p \rightarrow d + e^+ + \nu$	0,42	0,26	$6,0 \times 10^{10}$	$6,04 \times 10^{10}$
$p + p + e \rightarrow d + \nu$	1,44	1,44	$1,29 \times 10^8$	$1,43 \times 10^8$
${}^3He + p \rightarrow {}^4He + e^+ + \nu$	18,77	9,62	$1,23 \times 10^3$	$7,6 \times 10^3$
${}^7Be + e \rightarrow {}^7Li + \nu$	0,86 + 0,38	0,86 + 0,38	$4,18 \times 10^9$	$4,89 \times 10^9$
${}^8B \rightarrow {}^8Be + e^+ + \nu$	14,06	7,3	$3,83 \times 10^6$	$5,8 \times 10^6$
${}^{13}N \rightarrow {}^{13}C + e^+ + \nu$	1,20	0,71	$3,99 \times 10^8$	$6,1 \times 10^8$
${}^{15}O \rightarrow {}^{15}N + e^+ + \nu$	1,73	1,00	$3,09 \times 10^8$	$5,6 \times 10^8$
${}^{17}F \rightarrow {}^{17}O + e^+ + \nu$	1,74	1,00	$4,23 \times 10^6$	$5,39 \times 10^6$

**Table 1:** Energy and flux at the Earth according to two models of the reactions producing solar neutrinos.

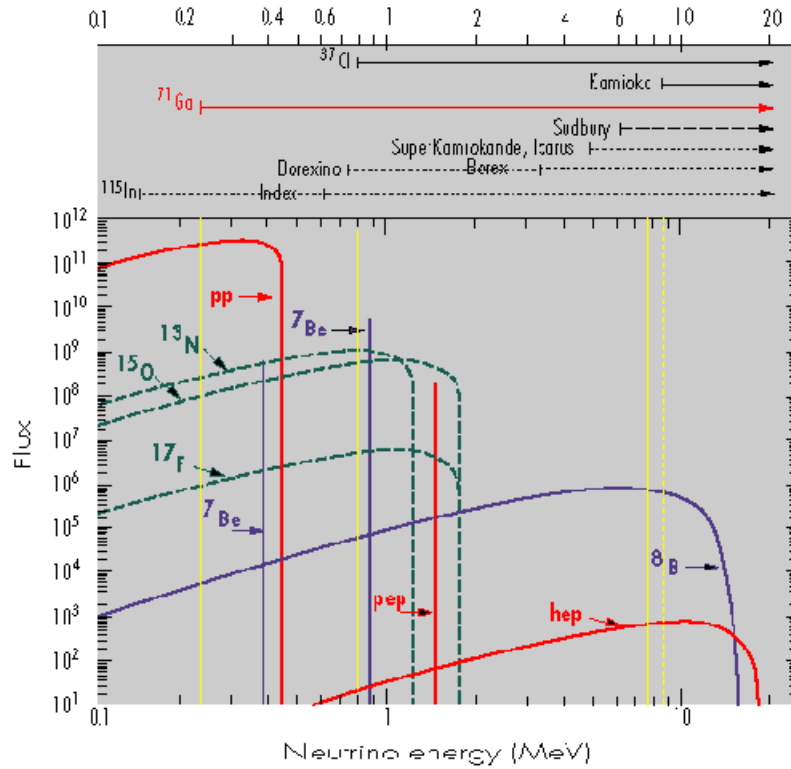


**Figure 3:** The energy spectrum of the reactions producing solar neutrino; on top some experiments and their energy threshold are shown.

Homestake (USA), started taking data in 1970; the gallium experiments, GALLEX (Gran Sasso, Italy) and Sage (Baksan, Russia) started in 1991. The experiment Kamiokande (Kamioka, Japan), designed for the study of proton decay but suitable for detecting solar neutrinos, has been upgraded (SuperK) and is still in operation.

The small cross section,  $\sigma \sim 10^{-46} m^2$  on average, requires to use a very large numbers of target nuclei. Since the  ${}^{37}Cl$  is sensitive almost exclusively to the high-energy neutrinos produced by the decay of  ${}^8B$ , with a flux at the Earth of  $\phi(\nu_e) \sim 6 \cdot 10^{10} m^{-2} s^{-1}$ , the number of expected

events is  $R = \phi(\nu_e) \cdot \sigma = 6 \cdot 10^{-36} s^{-1}$  per target nucleus. To have values  $R$  of the order of 1, a special unit has been introduced to calculate, or to measure, the number of neutrinos captured in a detector, the SNU (Solar Neutrino Unit), where  $1SNU = 1N\phi \cdot \sigma$  equals the capture of  $1\nu_e s^{-1}$  in a target consisting of  $N = 10^{36}$  target atoms. Given the much lower energy threshold, sensitive also to  $pp$  neutrinos, the  $Ga$  experiments have SNU values much higher than  $Cl$  experiments, even if with smaller masses. Finally, in radioactive detectors, because of the different lifetime  $\tau$  of the nuclei produced in  $\nu_e$  capture ( $\tau = 35$  days for  $Cl$ ,  $\tau = 11.4$  days for  $Ga$ ), the product nuclei are usually counted every 3 lifetimes. The results of a long series of measurements with  $^{37}Cl$  made by Homestake detector are show in Fig 4

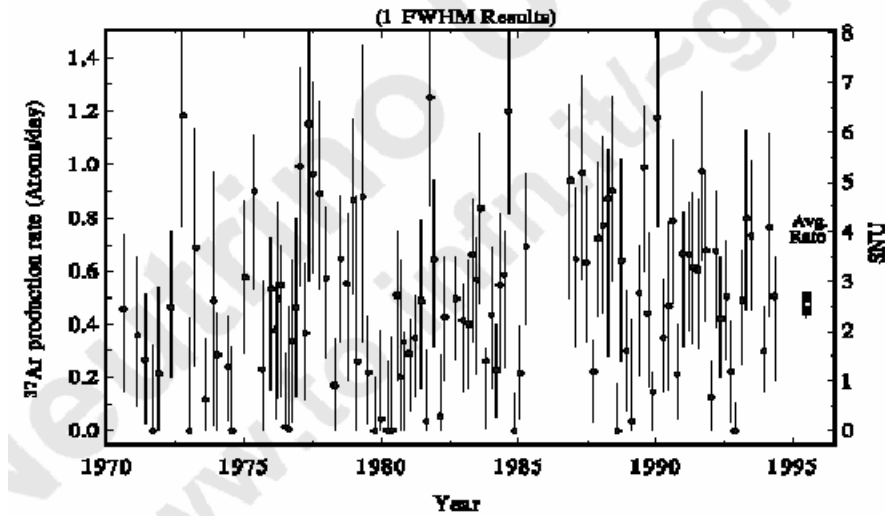
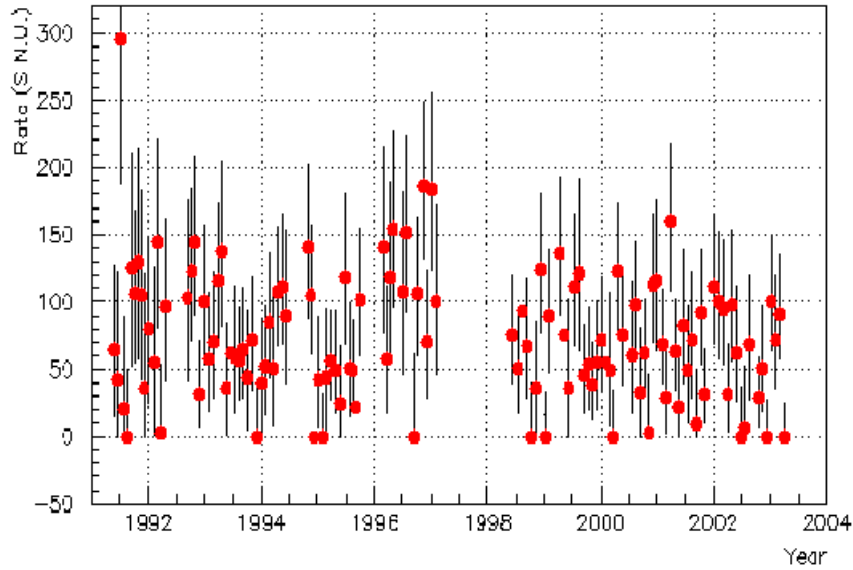


Figure 4: Measurements of Homestake

Reaction	$^{37}Cl$		$^{71}Ga$	
	capture (SNU)		capture (SNU)	
$pp$	0,0	0,0	70,8	71,1
$pep$	0,23	0,21	3,01	2,99
$^7Be$	1,12	0,99	34,4	30,9
$^8B$	6,15	4,06	14,1	10,77
$^{13}N$	0,10	0,10	3,77	2,36
$^{15}O$	0,34	0,37	6,03	3,66
$^{17}F$	3		0,06	
total	7,9	5,8	132	122,5
measurement	2,6 ± 0,16 ± 0,14 (Homestake)		70 ± 8 (Gallex) 72 ± 10 (Sage)	

Table 2: Number of catch (in two solar models) and measured in radiochemical experiments

In water Cherenkov experiments, neutrinos are detected in real time, and the main problem in such detectors is the high energy threshold, of the order of several MeV, so that these experiments can measure only the flux of neutrinos from  $^8B$ . However, they have the capability of directional



**Figure 5:** Measurements of Gallex

measurements and correlate, even if with relatively large angles, each event with the Sun's position in the sky. The Kamioka experiment has measured 0.31 events per day of neutrinos from  ${}^8B$ , corresponding to a fluence of  $[2.80 \pm 0.19(stat) \pm 0.33(Sist)]10^6 cm^{-2}s^{-1}$ , while a predicted value from the standard solar model is  $6.5 \times 10^6 cm^{-2}s^{-1}$

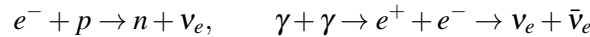
From table 2 one can note that the data from gallium experiments are almost in agreement with the predictions for  $pp$  and  $pep$  neutrino reactions that are certainly produced in the Sun because they are the starting reactions of hydrogen burning. Having a higher detection threshold, Homestake and Kamioka experiments are not able to detect  $pp$  and  $pep$  neutrinos, Kamioka only from those  ${}^8B$  and Homestake from  ${}^7Be$  and  ${}^8B$ . Also these experiments have measured a lower fluence than expected. This discrepancy was known in the past as the solar neutrino problem, because all the measured values were lower (in between 30% ~ 60%) compared with the expectations.

For years, various solutions have been proposed to solve the problem of the missing solar neutrinos, which can be grouped into two categories: astrophysical considerations to reduce the production of neutrinos in the Sun, or physical considerations on the properties of neutrinos as elementary particles. The solution came with the canadian experiment SNO (Sudbury Neutrino Observatory) based on a very large mass of heavy water as detector target, because neutrinos interact with the deuterium nuclei both via charged and neutral current interactions. The results of many years taking data show that the number of charged currents interactions is of order of 1/3 of the number of neutral current interactions in SNO. Since charged current interactions are due only to electron neutrinos, while neutral current interactions are due to neutrinos of any flavour, SNO confirm the neutrino oscillation mechanism: electron neutrinos are produced in the Sun in the quantity exactly predicted by the solar models but, on the way to the Earth, they oscillate into the other two flavours. Indeed the number of neutral currents interaction is in a very good agreement with the number expected from the hydrogen burning in the Sun, while the number of charged currents

interactions is only one third of the predictions, as observed also by all the previous experiments which are sensitive only to  $\nu_e$ . Thus, an astrophysical observation has a very important physical consequence: neutrino oscillations exist and are the explanation of the old solar neutrino problem.

### 3. Neutrinos from gravitational stellar collapse

The stellar collapse is unavoidable when the mass of the stellar core  $M_c$  exceeds the Chandrasekhar limit mass,  $M_{Ch} = 5.8Y_e^2 M_\odot \sim 1.44M_\odot$ , where  $M_\odot$  is the solar mass and  $Y_e$  the electron to baryon ratio in the core.  $M_c$  increases because of the burning of the Si shell around the core,  $M_{Ch}$  decreases because  $Y_e$  decreases in neutronization processes and pair annihilation.



In addition, gravity becomes overwhelming over thermal pressure because of the neutrino emission of these processes and the endothermic photodissociation process of iron nuclei:

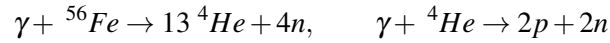


Table 3 gives the main characteristics of the neutrino emission, calculated for the gravitational collapse of a stellar core of  $2M_\odot$  mass, consisting of an inner iron core of  $1.82M_\odot$  and an oxygen envelop of  $0.18M_\odot$  around it. Three phases of the collapse are considered in this model:

1. Formation of the neutrino-sphere.
2. Accretion of the envelope on the core.
3. Kelvin cooling of the new born neutron star.

<i>Collapse's phases</i>	1	2	3
Total neutrino energy ( $10^{53}$ erg)	0,1	1,7	3
Average neutrino energy (MeV)	12	14	15
Time duration (s)	0,04	3,1	15

**Table 3:** Characteristics of the neutrino emission from the gravitational collapse of a  $2M_\odot$  stellar core.

In a stellar core with  $M_c \sim M_{Ch}$  there are of order of  $10^{57}$  electrons, so the maximum number of neutrinos emitted during neutronization processes is  $10^{57}$ . As their average energy is approximately  $10\text{MeV} \sim 10^{-12}\text{J}$ , the total energy emitted in this phase is about  $10^{45}\text{J}$ . The energy emitted by neutrinos during annihilation processes  $e^+e^-$  is about 20 to 30 times greater, that means  $3 \cdot 10^{46}\text{J}$ . For a collapse in the center of our Galaxy ( $d \sim 8.5\text{kpc}$ ) the flux of electron neutrinos to the Earth is :

$$\Phi(\nu_e, \bar{\nu}_e) = \frac{\Phi_0(\nu_e, \bar{\nu}_e)}{6 \cdot 4\pi d^2} \quad (3.1)$$

assuming energy equipartition among the 6 flavours. The main reactions for neutrino detection are electron scattering (3.2) and capture processes (3.3 and 3.4) with nucleons, namely:

$$\nu_e + e^- \rightarrow \nu_e + e^- \quad (3.2)$$

$$\bar{\nu}_e + p \rightarrow n + e^+ \quad (3.3)$$

$$\nu_e + n \rightarrow p + e^- \quad (3.4)$$

The corresponding cross sections are:

$$\sigma(\nu_e + e^-) = 10^{-44} (E_\nu / \text{MeV})^2 \text{cm}^2 \quad (3.5)$$

$$\sigma(\nu_e + n) = \sigma(\bar{\nu}_e + p) = 9 \cdot 10^{-44} (E_\nu / \text{MeV})^2 \text{cm}^2 \quad (3.6)$$

For  $E_\nu = 10 \text{MeV}$  the (3.6) is  $9 \cdot 10^{-42} \text{cm}^2$ , about 100 times higher than the (3.5) at the same energy; as a consequence, the capture processes are dominant compared to scattering. In addition, since neutrons are bound in the target nuclei of the detector, the neutrino-induced signal is integrated over the decay time of the compound nucleus, and (3.4) is not suited to study a neutrino burst that, according to most models, has a short duration. Because of the greater cross section, the interactions (3.3) of neutrinos with the free protons of the detector gives the main signal of a stellar collapse.

Since the energy threshold of reaction (3.3) is 1.8 MeV, the kinetic energy of the positron is  $E = E_\nu - 1.8 \text{MeV}$ ; however, positron annihilation with an electron of the detector returns 1 MeV. The neutron, after thermalization is detectable through the capture reaction with protons:

$$n + p \rightarrow d + \gamma \quad (3.7)$$

with the emission of the deuteron binding energy as a  $\gamma$  of energy  $E_\gamma = 2.2 \text{MeV}$  after an average delay  $\Delta t \sim 200 \mu\text{s}$  from the neutrino interaction. Because of the very low energy, both positron annihilation and the gamma from neutron capture are detectable in liquid scintillator but not in water. Therefore, the  $\bar{\nu}_e$  capture has a very good signature in scintillator: two signals produced in the reactions (3.3) and (3.7) in time sequence. For all the previously discussed motivations, the experiments for the detection of neutrinos from collapsing stars must have a hydrogen target, and the existing detectors use liquid scintillator (more sensitive) or water (bigger and cheaper).

Liquid scintillator detectors ( $C_n H_{2n}$ ). In these experiments, the detection threshold is limited only by the characteristics of the experiment and the background radiation (cosmic and environmental) of the laboratory where it is located, and usually is placed to values between 4 and 9 MeV. The energy deposited in the scintillator by the reaction (3.3) is the total energy of the positron, kinetics plus rest mass, because the  $2\gamma$  from electron annihilation are detectable. The interaction of a neutrino with energy  $E_\nu$  produces a visible energy  $E_{vis} = E_\nu - 0.8 \text{MeV}$  and has a good signature of electronic antineutrinos because of the delayed coincidence with the  $\gamma$  from (3.7).

Water detectors. Positrons from reaction (3.3) are detected by observing their Cherenkov light; the energy threshold is of order of 6 to 8 MeV. The visible energy in the detector is given by the kinetic energy of the positrons, since the  $2\gamma$  from electron annihilation are not detectable, as well

as  $\gamma$  from neutron capture (3.7). To the threshold of reaction (3.3), one should add the threshold for Cherenkov effect ( $\sim 0.25$  MeV for electrons in water), and the interaction of a neutrino with energy  $E_\nu$  releases the visible energy  $E_{vis} \sim E_\nu - 2MeV$ . In conclusion, the visible energy difference between the two types of detectors is:

$$E_{vis}^{scint} - E_{vis}^{water} = 1.2MeV \quad (3.8)$$

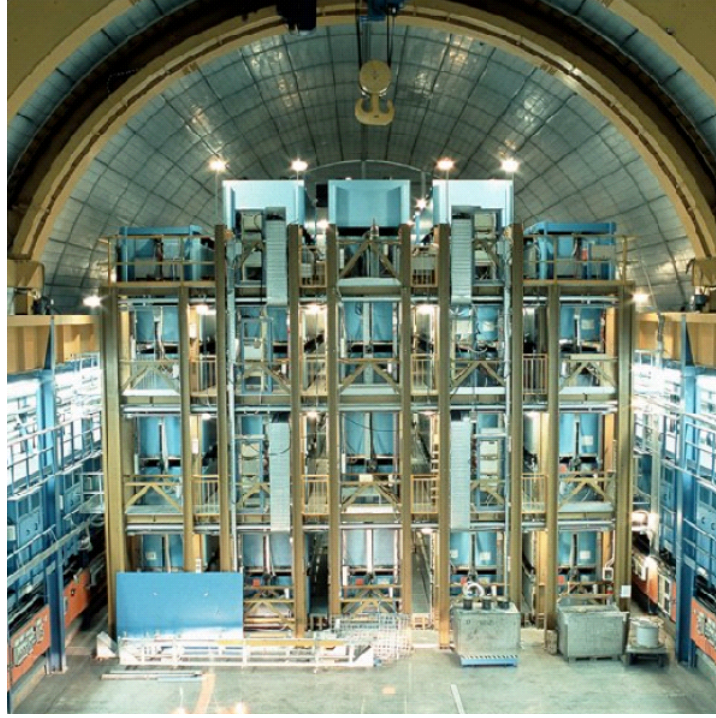
in favor of scintillator detectors for positron annihilation at rest, and increases for annihilation in flight. This difference could be a very important factor for the detection of low-energy neutrinos, emitted from a neutrinosphere at low temperature.

kT (MeV)	$E_{th}$ (MeV)	t(s)				
		0,01	0,1	1	10	> 25
3	5	0,15	2,55	9,3	24,4	35,3
	10	0,08	1,33	4,8	12,7	18,3
	15	0,02	0,39	1,4	3,7	5,4
	20	0,00	0,07	0,3	0,7	1,0
4	5	0,23	4,0	14,5	38	55
	10	0,17	3,0	10,9	29	41
	15	0,09	1,6	5,7	15	22
	20	0,04	0,6	2,2	5,9	8,5
5	5	0,31	5,3	19	51	73
	10	0,27	4,6	16,7	44	64
	15	0,19	3,2	11,7	31	45
	20	0,11	1,8	6,6	17	25

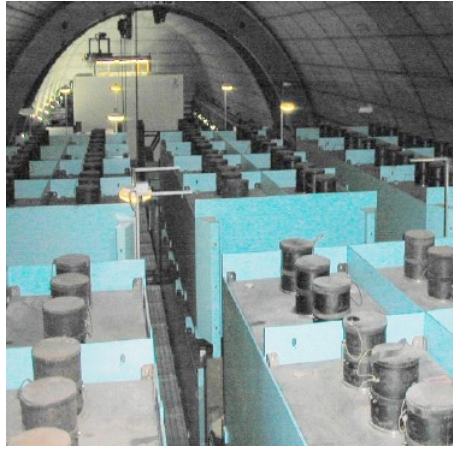
**Table 4:** Number of interactions  $(\bar{\nu}, p)$  in a 100 tons scintillation detector, calculated for a stellar collapse at the distance 10 kpc.

Table 4 gives the expected number of interactions recorded within the time  $t$  (seconds) in a detector of 100 tons of liquid scintillator with energy threshold  $E_{th}$  for a collapse with temperature  $T$  of the neutrinosphere at the distance  $d = 10$  kpc. The number of interactions  $(\bar{\nu}, p)$  is of the order of 0.5 per tons, assuming detection efficiency  $\varepsilon = 1$ . From this value, it is clear that only experiments with large sensitive volumes can detect neutrinos from a stellar collapse.

As an example, we discuss now the method to detect supernova neutrinos in the Large Volume Detector (LVD) of the Gran Sasso underground Laboratory in Italy. Shown in Fig. 6, the detector consist of 840 scintillation counters,  $1.5m^3$  each, inserted in modules holding 8 counters each. The modules are grouped and stacked together to form three towers of 35 modules each. The scintillator of each counter (1.2 tons) is watched from the top by 3 PMT's (15 cm diameter each) as shown in Fig. 7. The energy threshold of each counter is set between 4 and 6 MeV, depending on its exposure to the radioactive background from the rock. A threshold of 0.8 MeV is enabled for a time  $\Delta t = 10^{-3}s$  after the main neutrino interaction, to detect  $\gamma$  from neutron capture (3.7).



**Figure 6:** Large volume detector LVD experiment at Gran Sasso



**Figure 7:** Scintillator of each counter is watch by 3 PMT's

In a liquid scintillation detector, in addition to neutrino interactions with protons and electrons, there are also neutral and charged currents interactions with the carbon nuclei of the scintillator that do not occur in water, because water has no carbon nuclei. The Quasi-thermal Fermi-Dirac neutrino energy spectra from a collapsing star are shown in fig 8, where  $\nu_{\mu,\tau}, \bar{\nu}_{\mu,\tau}$ .

The neutrino reactions detectable in LVD are the following:

1. Inverse beta decay:  $(\bar{\nu} + p \rightarrow n + e^+)$ . Both products of this interaction are detectable, namely: a positron by the first pulse followed by a delayed pulse from neutron capture  $n + p \rightarrow d + \gamma$ . These gamma are detected in a time window of 1 ms during which the detection threshold is

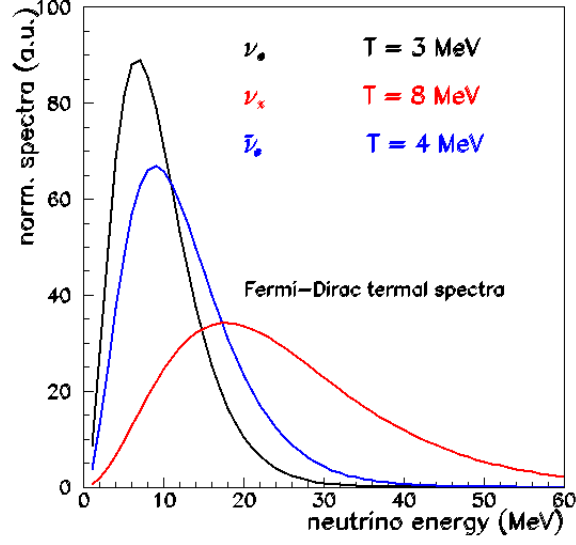


**Figure 8:** Energy spectrum of neutrinos from collapse expected in LVD

lowered in energy to 0.8 MeV. The reaction produces the largest number of events in the detector and gives a very clear anti-electron neutrino signature.

2. Neutrino - electron scattering:  $\nu_e + e^- \rightarrow \nu_e + e^-$ . This interaction produces a single pulse in one scintillation counter.

3. Neutral current interactions:  $\nu_{e,\mu,\tau}(\bar{\nu}_{e,\mu,\tau}) + {}^{12}\text{C} \rightarrow \nu_{e,\mu,\tau}(\bar{\nu}_{e,\mu,\tau}) + {}^{12}\text{C}^*$ , followed by the process of carbon de-excitation:  ${}^{12}\text{C}^* \rightarrow {}^{12}\text{C} + \gamma$ , being the  $\gamma$  emitted with energy 15.1 MeV. This process is identified with good precision: the released  $\gamma$  energy from carbon is monoenergetic and it is observable in a well-defined energy range in a single counter.

4. Charge current interactions:  $\nu_e + {}^{12}\text{C} \rightarrow {}^{12}\text{N} + e^-$  (with an energy threshold of 17.3 MeV) followed, with an average delay  $\tau = 15.9\text{ms}$ , by the  $\beta$  decay of nitrogen  ${}^{12}\text{N} \rightarrow {}^{12}\text{C} + e^+ + \nu_e$ .

5. Charge current interactions:  $\bar{\nu}_e + {}^{12}\text{C} \rightarrow {}^{12}\text{B} + e^+$  (with a energy threshold of 14.4 MeV) followed, with an average delay  $\tau = 29.4\text{ms}$ , by the  $\beta$  decay of boron  ${}^{12}\text{B} \rightarrow {}^{12}\text{C} + e^- + \bar{\nu}_e$ .

The signature of both reactions [4] and [5] is given by two pulses in time coincidence in the same counter.

The number of interactions expected for a collapse at the galactic center is generally estimated assuming equipartition of energy among the six neutrino species. However neutrinos oscillate during the journey from the star to the detector, then the number could change, and reactions [4] and [5] can produce a greater number of interactions. This could provide an indirect opportunity to study neutrino oscillations from a stellar gravitational collapses. Also information on neutrino mass can eventually be obtained from the time delay of massive particles compared to the arrival times of particles with lower or zero mass. For example, neutrinos of energy  $E_1$  and  $E_2 > E_1$  emitted simultaneously from the source, after having travelled for the distance  $d$ , are separated by a time interval:

$$\Delta t = (d/2c)(m_\nu c^2)^2 \cdot (E_1^2 - E_2^2) \quad (3.9)$$

The delay between neutrinos of mass  $m_\nu$  and massless particles is given by:

$$\Delta t = 0.5 \frac{d}{10kpc} \cdot \left( \frac{100MeV}{E_\nu} \right)^2 \cdot \left( \frac{m_\nu}{10eV} \right)^2 \quad (3.10)$$

In conclusion, if the distance of the supernova is known, by measuring the delay  $\Delta t$  (equivalent to having measured the velocity  $v = d/\Delta t$ ) and the neutrino energy  $E_\nu$ , one can estimate the neutrino mass provided the experiments has good time and energy resolution.

#### 4. Identification of a neutrino burst

Neutrino detectors are located at great depths underground to reduce the background of cosmic radiation, and improve the identification of the weak signal induced by neutrinos from a stellar collapse; only muons can penetrate several kilometers of rock, but they are easily identified by their large energy losses in the detector. The neutrino signal is small, and can be confused with radioactive background or with products of muon interactions in the rock surrounding the detector. For this reason, a first step is to analyze only clusters of rare events, statistically significant as compared to similar groups of row events; in a second step, after the neutrino burst has been identified, a check on the characteristics of individual interactions is made. As an example, we discuss the procedure followed in the old experiment LSD, similar to that of many recent neutrino detectors.

Suppose that in an underground laboratory, the background counting rate has a frequency  $f$  (Hz), and that the probability to record  $m$  events in a time  $\Delta t$  agrees to a Poisson distribution with average value  $f \Delta t$ . The imitation frequency  $F_{im}$  of a package of at least  $(m-1)$  pulses in a time interval  $\Delta t$ , after a trigger pulse, is given by:

$$F_{im} = f \sum_{k=m-1}^{\infty} P(k, \Delta t) = f \sum_{k=m-1}^{\infty} \frac{(f\Delta t)^k}{k!} \cdot e^{-f\Delta t} \quad (4.1)$$

For example, figures (9) and (10) show the experimental distributions of groups of pulses of different multiplicity  $m$ , recorded in time intervals in the range from  $10^{-3}s$  to  $2 \cdot 10^2s$  for the LVD experiment, indicating a good agreement with the distributions calculated from the background (4.1) and, therefore, not showing any statistically significant burst. The curves, calculated according to Poisson distributions, agree very well with the experimental distributions of events. On the contrary, if a group of  $m$  data detected in a time interval  $\Delta t$  had a frequency much lower than a pre-set value (e.g. 0.1 per year), the corresponding group of pulses would undergo a complete physical analysis to ensure its consistency with the characteristics of a real burst of neutrinos from a stellar collapse.

The second level of analysis consists in checking the following characteristics of the burst of pulses:

1. Topological distribution of pulses. A real physical event must have a fairly uniform spatial distribution in the volume of the detector. In background events, due to shielding effects, the interactions occur more frequently in the surface than in the internal counters, shielded by the surface ones.

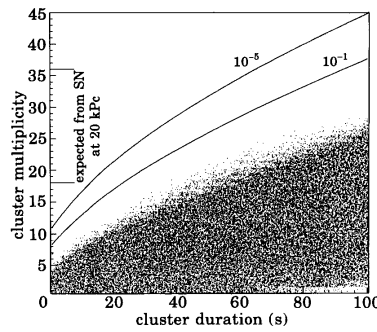


**Figure 9:** Distribution of groups of pulses in time

2. Energy Distribution. A real physical event must have a Fermi-Dirac energy distribution; the background events have a completely different distribution, as shown in figure (11).

3. Delayed low energy pulse. These events are typical of electron antineutrino interactions in the scintillator, due to the two pulses from interactions (3.3) and (3.7).

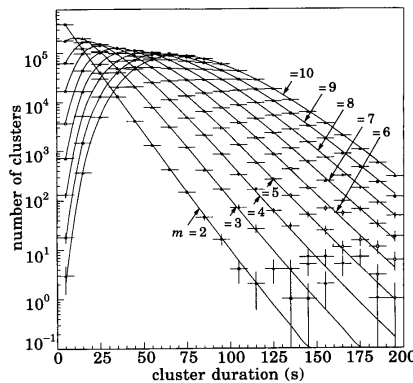


**Figure 10:** Distribution of groups of pulses in a tower of LVD

Figure (12) gives the number of interactions in LVD of antineutrinos from gravitational stellar collapses at different distances from the Earth. One can see that the LVD experiment is sensitive up to the distance of the Magellanic Clouds, and is always sensitive also to nearby stellar collapses without the data acquisition system being saturated by the large number of interactions. Finally, it is expected that the neutrino burst from a stellar gravitational collapse arrives to the Earth several hours (or even days) before the optical brightness of the star increases. This is due to the fact that neutrinos are emitted at the time of the core collapse, while the increment in brightness is due to the expansion of the envelope after the collapse. Thus, an immediate recognition of the neutrino burst not only can be confirmed by subsequent observations in the electromagnetic domain, but also facilitate the search for supernovae in Astronomical Observatories, allowing the detailed study of the early stages of evolution of the phenomenon.

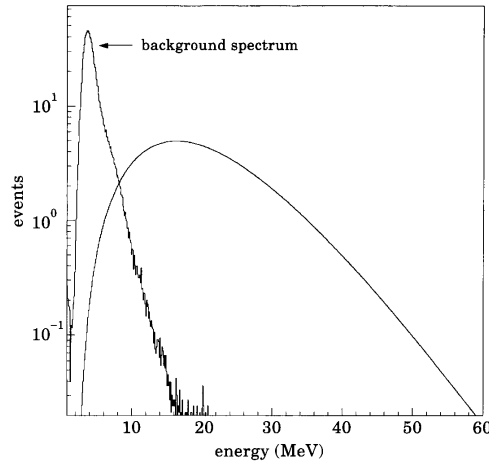


**Figure 11:** Fermi-Dirac and background distributions of pulses measured in LVD.

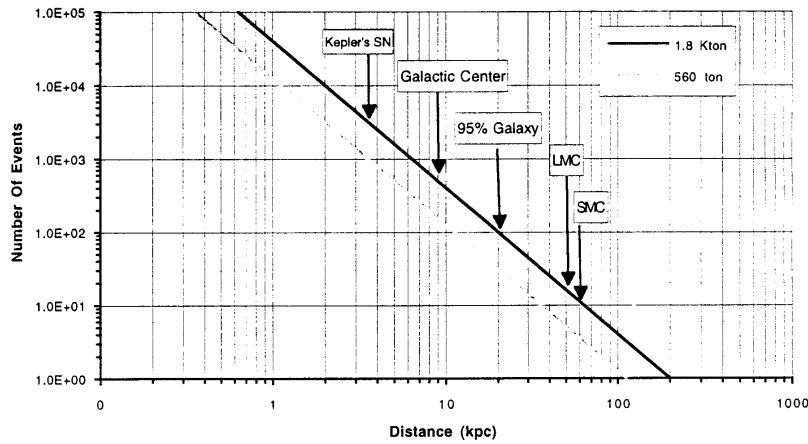


**Figure 12:** Neutrinos sensitivity from stellar collapses at the LVD.

### 5. Neutrinos from Supernova 1987 A

On february 23, 1987 at 10h33m Universal Time, the canadian astronomer Ian Shelton, at the Observatory of Las Campanas in Chile, observed a supernova of visual magnitude  $m_v \sim 6$  in the Magellanic Clouds; from previous astronomical observations it has been shown that the star had a magnitude  $m_v \sim 12$  at 01h55m the same day. The explosion of the first supernova visible to naked eye of the modern era occurred in this interval of about 8 hours. The pre-supernova was a blue supergiant (B3 Ia) of mass between 20 and 25  $M_\odot$ , probably in a binary system; many astronomical observations show that this was a peculiar supernova, for example:

1. The explosion occurred in a small irregular galaxy, with a metal abundance much lower than what it is expected for population I stars, which are believed to be progenitors of type II supernovae.
2. The pre-supernova was a blue supergiant, not a red one, contrary to all previous predictions

from models of stellar evolution.

3. It had an absolute magnitude at maximum much lower than all other supernovae of the same type.

4. The explosion occurred in a binary system or, may be, in a system made by 3 or more stars, in which the mass transfer during the explosion may have altered the mechanism of gravitational collapse and neutrino emission expected by the existing models, all based on the explosion of single stars, without rotation or magnetic fields.

5. Two distinct neutrino burst, separated 4.7 hours one from the other, were observed.

Here, we will discuss briefly only this last point. At the time of the explosion, a burst of 5 interactions was recorded in real time by the neutrino experiment LSD (Liquid Scintillation Detector) designed to search for neutrinos from gravitational stellar collapses in our Galaxy in the underground Mont Blanc Laboratory (Italy). Two weeks later, after extracting the signal from the raw data, a second burst was found in other underground detectors: two water Cherenkov detectors (Kamiokande in Japan, and IBM in USA) designed to study proton decay, and a liquid scintillation detectors in Baksan (Russia) designed to detect neutrinos from collapsing stars and to study cosmic radiation. The main characteristics of these underground detectors are given in table (5), together with their observations of neutrinos from SN 1987A.

<i>Experiment</i>	<i>Mont Blanc</i>	<i>Baksan</i>	<i>Kamioka</i>	<i>IMB</i>
<i>Characteristics</i>				
Depth (m.a.e.)	5200	850	2500	1570
Active mass (tonnes)	$C_nH_{2n}$ (90)	$C_nH_{2n}$ (200)	$H_2O$ (2140)	$H_2O$ (5000)
Threshold at 50% (MeV)	5 - 6	9 - 10	9 - 10	25
Sensitivity (ph / MeV)	15	3 - 5	3,4	1,2
Background ( $\mu$ /hour)	3,5	$10^6$	$10^3$	$10^4$
No of detected neutrinos	5	5 (+2)	11 (+2)	8
Detected energy (MeV)	5,8 - 7,8	12 - 23	8 - 35	19 - 39
Start of the event (TU)	2h52m37s	7h36m06s	7h35m35s	7h35m41s
Duration of the event (s)	7	9	12	6
Temporal precision	$\pm 2$ ms	(-54, +2) s	$\pm 1$ min	$\pm 5$ ms

**Table 5:** Main features of the experiments that showed neutrinos from SN 1987A. The depth is in meters of water equivalent sensitivity in photoelectrons per MeV. Kamioka and Baksan experiments have also observed two events in time coincidence with the event of Mont Blanc.

It is not clear how to find an explanation for the two neutrino observations, but it has been shown that, from the experimental point of view, they are not in contradiction. Indeed, the 5 interactions observed in the Mount Blanc liquid scintillator with visible energy in the range (5.8 to 7.8) MeV, correspond in water to energies in the range (4.6 to 6.6) MeV considering the positron annihilation at rest, and (4-6) MeV considering annihilation in flight. Due to the different detection threshold of the other experiments, the low-energy Mont Blanc event is not detectable, or only marginally detectable in these experiments. Thus, it is not surprising that the event observed in Mont Blanc has not produced significant signals in experiments of larger volume but with lower sensitivity because of their higher detection threshold. In addition, a correlation analysis of the

experimental data of all these detectors has shown a clear excess of coincidences among all the experiments at the Mont Blanc time. It is surprising that four experiments (one in Europe, one in USA, one in Japan and the other in Russia) have observed an excess of coincidences at the Mont Blanc time, when a supernova exploded and not at other times. A new model, recently proposed and based on the fragmentation of the core because of rotation, can probably explain the emission of neutrinos for times much longer than the predictions of previous models. But we need a new galactic supernova to check the model.